

## First-order transition to oscillation death in coupled oscillators with higher-order interactions

Richita Ghosh,<sup>1</sup> Umesh Kumar Verma,<sup>2</sup> Sarika Jalan,<sup>2</sup> and Manish Dev Shrimali<sup>1,\*</sup>

<sup>1</sup>*Department of Physics, Central University of Rajasthan, Rajasthan, Ajmer-305 817, India*

<sup>2</sup>*Complex Systems Laboratory, Department of Physics, Indian Institute of Technology Indore, Khandwa Road, Simrol, Indore-453 552, India*



(Received 9 June 2023; accepted 11 September 2023; published 6 October 2023)

We investigate the dynamical evolution of Stuart-Landau oscillators globally coupled through conjugate or dissimilar variables on simplicial complexes. We report a first-order explosive phase transition from an oscillatory state to oscillation death, with higher-order (2-simplex triadic) interactions, as opposed to the second-order transition with only pairwise (1-simplex) interactions. Moreover, the system displays four distinct homogeneous steady states in the presence of triadic interactions, in contrast to the two homogeneous steady states observed with dyadic interactions. We calculate the backward transition point analytically, confirming the numerical results and providing the origin of the dynamical states in the transition region. The results are robust against the application of noise. The study will be useful in understanding complex systems, such as ecological and epidemiological, having higher-order interactions and coupling through conjugate variables.

DOI: [10.1103/PhysRevE.108.044207](https://doi.org/10.1103/PhysRevE.108.044207)

### I. INTRODUCTION

The dynamics of interacting systems are usually modeled using the concept of complex networks [1]. The units of each system are denoted as nodes, and the interactions by links joining the nodes form networks. Most of the studies on networks deal with pairwise interactions between the nodes. However, such a simplified version of pairwise interactions is not justified while dealing with systems such as those formed by coauthors of research articles, multiple species competing for food in an ecosystem, or phenomena of diseases and rumors in society, etc. In nature, systems such as those governed by social [2,3], biological [4,5], neuroscience [6,7], or ecological dynamics [8,9] are reigned by group interactions. The mathematical framework of pairwise links in networks is insufficient to represent such systems. Simplicial complexes are one of the simplest candidates for encoding higher-order interactions mathematically. A simplex of  $N$  dimensions can be conceptualized as a set of  $(n + 1)$  nodes.

The node set  $\mathcal{S}$  may be written as  $\mathcal{S} = [x_0, x_1, \dots, x_n]$ , in which the individual elements of the set denote each vertex (node) of the simplex. A one-dimensional simplex represents a link between two nodes, while a two-dimensional simplex represents a triangle (denoting interaction between three nodes). Hence, simplicial complexes may be considered topological constructions constituting simplices of different dimensions [10].

Further, dynamical processes evolving on complex networks have been shown to exhibit collective emergent phenomena such as synchronization [11], self-organization [12], oscillation quenching [13], and chimera states [14]. Among these, oscillation suppression in dynamical systems is a well documented and interesting behavior arising due to

interactions in complex systems. The onset of suppression of oscillations has been observed through various coupling schemes such as mean-field diffusive [15], through dissimilar or conjugate [16] and environmental variables [17], and with attractive-repulsive links [18] in networks of both limit-cycle and chaotic oscillators.

Suppression of oscillations can occur through two routes: amplitude death (AD) [19] and oscillation death (OD) [20]. For AD the coupled oscillators stabilize to a common steady state which is also a stable global fixed point of the system, whereas in OD they can settle to different fixed points referred to as in-homogeneous (IHSS) steady state via symmetry-breaking bifurcation or to a same fixed point referred as homogeneous (HSS) steady states. The suppression of oscillations is relevant in various places, for instance, in medical science in controlling diseases like Parkinson's and Alzheimer's. Other examples include neuron models [21], lasers [22], and climate systems [23].

Further, the transition from oscillations to the quenching of oscillations may be either continuous and smooth or discontinuous and explosive. There have been extensive studies on first-order transition to synchronization, referred to as explosive synchronization [24,25], explosive percolation [26], and explosive death [27], on networks with dyadic interactions. Bi *et al.* reported the phenomenon of explosive death in a network of Stuart-Landau oscillators coupled through pairwise similar variables [28]. Explosive death (ED) [29–35] and semiexplosive death [36] were also observed in a network of conjugate-coupled limit-cycle oscillators. The phenomenon of ED brings with it a hysteresis or bistable region, i.e., a region in the parameter space where the oscillatory and the steady states coexist. Such bistability has been observed in several physical [37] and chemical systems [38].

With the advent of studies on higher-order interactions, collective dynamics, such as synchronization [39–44], and chimera states [45] have been reported for coupled

\*shrimali@curaj.ac.in

dynamics on simplicial complexes. In explosive transitions to synchronization, systems evolving on simplicial complexes have been shown to suddenly experience a transition to synchronization from an incoherence state and vice versa [46]. Further, multilayer networks of simplicial complexes have exhibited multiple routes to explosive synchronization [47,48]. Recently, a sudden transition to antiphase synchronization on adaptive simplicial complexes has also been explored [49]. Recently, amplitude death has also been reported in networks with additive triadic conjugate interactions [50].

Extensive studies have been conducted on mathematical models having dissimilar or conjugate variables couplings capturing pairwise interactions [51]. A few examples of situations that demand conjugate coupling include electronic circuits [52], ecological models [53], and models of chemical kinetics [54]. In ecological networks, multiple species compete with each other for food. The phenomenon of cross-predation within ecological systems occurs when the predator of one predator-prey system consumes the prey of another similar system. Such networks cannot be modeled accurately by dyadic or pairwise links. Hence, models simulated on networks with higher-order interactions lead to a more accurate representation of such complex systems. In another scenario, interactions between the chemical film on a metal surface and the metal ions have been studied using pairwise conjugate coupling. Nevertheless, due to the presence of some impurities in the chemical film, the impurities may also interact with the metal ions or the film itself. The products of these undesired reactions may further interact with the original chemical species or among themselves. Such types of interactions will require mapping beyond pairwise links, and therefore models with conjugate higher-order interactions should be considered for an accurate representation of such phenomena.

In this study we extend the mathematical framework of triadic interactions as proposed by Gambuzza *et al.* [55] to induct conjugate coupling or coupling through dissimilar variables. We investigate the effect of such a higher-order conjugate coupling on Stuart-Landau oscillators and discover a first-order phase transition from oscillatory to steady state in the presence of triadic interactions instead of the continuous second-order phase transition observed with only pairwise interactions. We perform linear stability analysis for all the fixed points and derive the condition for the transition point from oscillation to steady state to further confirm the numerical results. The robustness of our model has been checked against the application of a noise signal of appropriate strength.

### A. Model

Our model system, with 1-simplex (pairwise) and 2-simplex (triadic) interactions with conjugate or dissimilar variables, has been mathematically formulated in the following way:

$$\begin{aligned} \dot{\mathbf{X}}_i &= \mathbf{F}(\mathbf{X}_i) + \frac{\epsilon_p}{N} \sum_{j=1}^N \mathbf{f}_p(\mathbf{X}_i, \mathbf{X}_j^*) \\ &+ \frac{\epsilon_h}{N^2} \sum_{j=1}^N \sum_{k=1}^N \mathbf{f}_h(\mathbf{X}_i, \mathbf{X}_j^*, \mathbf{X}_k), \end{aligned} \quad (1)$$

where  $\mathbf{X}_i^*$  is the conjugate variable of the state variable  $\mathbf{X}_i$ . The  $w$ -dimensional state vector  $\mathbf{X}_i$  denotes the dynamics of each unit  $i$  where  $i = 1, 2, \dots, N$ . The dynamics of each isolated node are assumed to be identical and described by  $F : \mathbb{R}^w \rightarrow \mathbb{R}^w$ ,  $f_p : \mathbb{R}^{2 \times w} \rightarrow \mathbb{R}^w$ , and  $f_h : \mathbb{R}^{3 \times w} \rightarrow \mathbb{R}^w$  denotes the conjugate coupling functions for the 1-simplex and 2-simplex interactions, respectively.  $\epsilon_p$  illustrates the coupling strength for the pairwise interactions and  $\epsilon_h$  for the triadic ones.

We consider a globally connected network of  $N$  Stuart-Landau (*SL*) limit-cycle oscillators, interacting with each other through pairwise and triadic interactions. The equations governing the dynamics of the system are

$$\begin{aligned} \dot{x}_i &= (1 - x_i^2 - y_i^2)x_i - \omega y_i + \frac{\epsilon_p}{N} \sum_{j=1}^N (y_j - x_i) \\ &+ \frac{\epsilon_h}{N^2} \sum_{j=1}^N \sum_{k=1}^N (x_j y_k^2 - x_i^3), \\ \dot{y}_i &= (1 - x_i^2 - y_i^2)y_i + \omega x_i + \frac{\epsilon_p}{N} \sum_{j=1}^N (x_j - y_i) \\ &+ \frac{\epsilon_h}{N^2} \sum_{j=1}^N \sum_{k=1}^N (y_j x_k^2 - y_i^3), \end{aligned} \quad (2)$$

with  $i = 1, 2, \dots, N$ , and  $\omega$  is the intrinsic frequency of the oscillators. The  $N$  nodes in the network are coupled to each other by ‘‘conjugate’’ variables.  $\epsilon_p$  and  $\epsilon_h$  are the coupling strengths associated with 1-simplex (pairwise interaction) and 2-simplex (triadic interaction), respectively.

The dynamical equations [Eq. (2)] have been solved numerically using the *RK4* method with a step size of 0.01 after removing transients of the order of  $10^5$ . The initial conditions were randomly chosen within the interval  $[-1, 1]$ . To characterize the nature of the transition from the oscillatory state to the death state in our model system, we adopt an order parameter in terms of average amplitude [56],

$$A(\epsilon) = \frac{a(\epsilon)}{a(0)},$$

where  $a(\epsilon) = \sum_{i=1}^N \frac{1}{N} (\langle x_{i,\max} \rangle_t - \langle x_{i,\min} \rangle_t)$ , with  $\langle \dots \rangle_t$  representing the average over long time.  $a(\epsilon)$  is a measure of the difference of the global maxima and minima of the time-series data of all the oscillators, computed over a long time after discarding a sufficient amount of transients at a particular coupling strength  $\epsilon$ .  $a(0)$  is the average amplitude at  $\epsilon = 0$ . The normalized order parameter  $A(\epsilon)$  is greater than 0 when the coupled system is in the oscillatory state; however, when the system attains a steady state,  $A(\epsilon) = 0$ . This order parameter has been calculated adiabatic by varying the value of  $\epsilon$  ( $\epsilon_p$  or  $\epsilon_h$ ) in forward and backward continuation. This process is termed ‘‘adiabatic’’ since the system’s state in the previous run is used as the initial conditions of the next run of the simulations [27]. During the forward continuation process, the coupling strength  $\epsilon$  increases slowly in steps of  $\delta\epsilon$ . When a specified value of  $\epsilon$  is reached, the backward continuation process starts where  $\epsilon$  is now decreased slowly in a similar fashion and continued until the minimum value of  $\epsilon$  is reached.

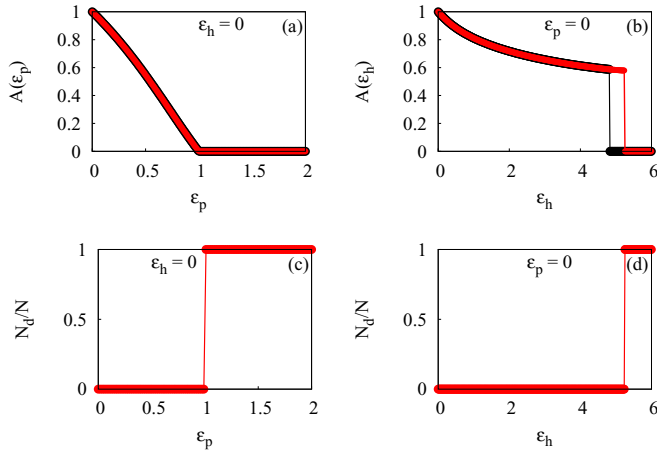


FIG. 1. Amplitude order parameter  $A$  for (a) pairwise and (b) triadic interactions. The fraction of oscillators  $N_d/N$  is calculated for (c) 1-simplex interactions and (d) 2-simplex interactions. Here,  $\omega = 1$  and  $N = 100$ . The curves in red have been computed in forward continuation, and the black ones have been calculated in backward continuation.

**B. Numerical results for 1-simplex (dyadic) interactions**

We set  $\epsilon_h = 0$  in Eq. (2) to investigate the dynamics with only pairwise interactions. The coupling strength  $\epsilon_p$  varies adiabatically in steps of 0.02 in both forward and backward continuation. Figure 1(a) exhibits a second-order transition from oscillation to death of oscillations. The order parameter  $A(\epsilon_p)$  gradually decreases to zero, indicating suppression of oscillations in the system with a gradual increase in coupling strength. The forward and backward continuations show no change in the transition point, i.e., in both cases the critical value of  $\epsilon_p$  remains the same, as observed in Fig. 1(a). Hence, in the presence of only conjugate dyadic links, the system shows a continuous and reversible second-order phase transition from oscillation to the death state, without any hysteresis via supercritical Hopf bifurcation.

Next we discuss the dynamics of the system at the transition points. The bifurcation diagram for the  $SL$  oscillators with pairwise interactions has been illustrated in Fig. 2(a). Here a supercritical Hopf bifurcation destroys the oscillations from the stable limit cycle, displayed in green. A subsequent supercritical pitchfork bifurcation also occurs immediately, giving rise to the two stable solutions which have been displayed in red in Fig. 2(a).

**C. Numerical results for 2-simplex (triadic) interactions**

Next we consider the case of  $\epsilon_p = 0$  in Eq. (2), i.e., only the triadic interactions are prevalent in the model.  $\epsilon_h$  is varied in an adiabatic manner, from 0 to  $\epsilon_{h,max}$  in steps of  $\delta\epsilon_h = 0.02$  for the forward continuation. During this process the magnitude of the order parameter  $A(\epsilon_h)$  suddenly drops to 0, indicating an explosive transition from oscillatory to steady state, as shown in Fig. 1(b). The transition point from oscillatory to death state occurs for a critical  $\epsilon_h = 5.2$ . For the backward continuation process, we decrease  $\epsilon_h$  from  $\epsilon_{h,max}$  to 0 similarly and observe that the amplitude order parameter jumps from 0 to nonzero values at around  $\epsilon_h = 4.82$ . Hence, it is clear that the forward

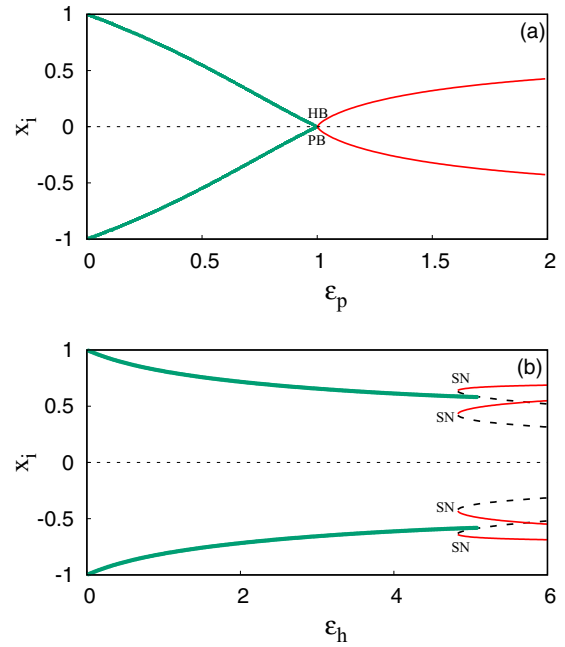


FIG. 2. The bifurcation diagram of the coupled  $SL$  oscillators is plotted. (a) For 1-simplex interactions and (b) for 2-simplex interactions. The red solid lines correspond to the stable fixed points, the dashed black lines correspond to the unstable ones, and the green solid lines indicate the oscillatory solutions from the stable limit cycle.  $i = 1, 2, \dots, N$ .

and backward transition points do not coincide. This indicates a hysteresis region in the parameter space, i.e., a bistable region where both oscillatory and HSS states coexist. Such an abrupt and sudden transition with a hysteresis region can be categorized as a first-order transition.

To investigate whether all the oscillators are going to death state simultaneously or some oscillators may attain death state faster than others, we define a parameter  $N_d/N$ , where  $N_d$  is the number of oscillators going to steady state and  $N$  is the total number of oscillators. This parameter is also computed in a similar adiabatic way of forward continuation, as described previously. Figures 1(c) and 1(d) depict the abrupt jump from 0 to 1 for pairwise and triadic interactions, respectively. This indicates that the oscillators attain a death state simultaneously after crossing a threshold value of  $\epsilon_h$ . We note that this value of  $\epsilon_h$  agrees well with our results for forward continuation.

The dynamics at the transition point for the triadic interactions differ from that of the 1-simplex ones. The oscillations of the system remain in complete synchronization until a critical value of  $\epsilon_h$  is reached. At this point the system stabilizes to newly created fixed points through saddle-node bifurcations. Due to the bifurcations, two pairs of stable and unstable fixed points appear. The oscillations from the stable limit cycle continue and collide with the unstable fixed points. This leads to the disappearance of the limit cycle, and the system settles down to any of the stable fixed points, depending on the initial conditions. This scenario of a stable limit cycle being destroyed by an unstable fixed point is the mechanism of a

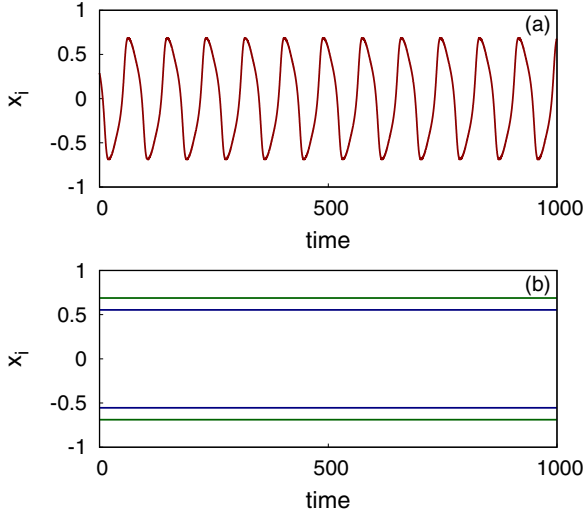


FIG. 3. Time series of the coupled *SL* oscillators with 2-simplex interactions is plotted. (a) At  $\epsilon_h = 2.45$ , i.e., in the oscillatory region (b) at  $\epsilon_h = 6.11$ , i.e., at steady-state region, one set of fixed points ( $x_i \approx \pm 0.55$ ) which are displayed in dark purple and the other set of fixed points ( $x_i \approx \pm 0.68$ ) which are displayed in dark green also appear, depending on the choice of initial conditions for the same value of  $\epsilon_h = 6.11$ . The other parameters are  $\omega = 1$ ,  $N = 100$ , and  $i = 1, 2, \dots, N$ .

subcritical Hopf bifurcation. The entire dynamics of the model system at the transition point are illustrated in Fig. 2(b).

Figure 3 demonstrates the transition of the model system from oscillation to oscillation-quenching. The system shows periodic and completely synchronous oscillations [Fig. 3(a)] for coupling strengths below the critical value of  $\epsilon_h$  for which the transition to a steady state takes place. The system goes to a fixed point as  $\epsilon_h$  increases beyond this point. Depending on the choice of initial conditions, the oscillators may settle down to any of the four homogeneous steady states shown in Fig. 3(b). Figure 3(b) exhibits the fixed points  $x_i^* \approx \pm 0.55$ , displayed in dark purple, and  $x_i^* \approx \pm 0.68$ , illustrated in dark green. It is interesting to note that the system has a kind of mirror-image symmetry. That is to say, the dynamics occurring in the phase space above the origin are mirrored in the phase space below the origin. Figure 4(a) displays the basin of attraction at the hysteresis region. The numerical results have been calculated for  $\epsilon_h = 5.0$ . since the hysteresis region stretches from  $\epsilon_h \approx 4.82$  to  $\epsilon_h \approx 5.25$ . Here we confirm the presence of bistability through the two regions illustrated in the figure. The pink region corresponds to the initial conditions triggering the oscillatory state, and the light blue region denotes the ones for the death state. The initial conditions  $x_i$  and  $y_i$  have been varied from  $-1$  to  $1$ . In Fig. 4(b) the basin of attraction for the four fixed point attractors in the system is displayed. The value of the coupling strength has been fixed at around 5.6, since we are exploring the basin after the system achieves a steady state. In this figure each of the four differently shaded (colored) regions is populated by the initial conditions for the four different fixed points that the oscillations settle down to during the steady state. In Fig. 4 we consider  $x = x_i$  and  $y = y_i$ , since the system is in either complete synchronization or HSS in the hysteresis

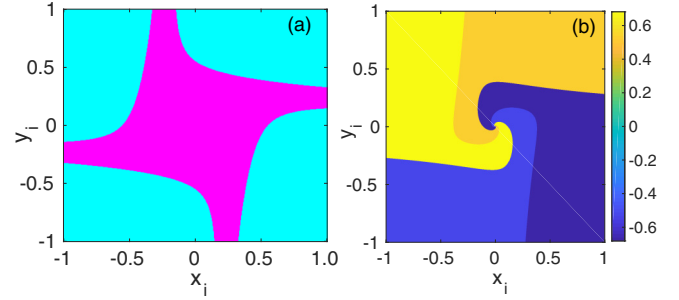


FIG. 4. Basin of attraction illustrating the stable states in the system. (a) At the hysteresis region  $\epsilon_h = 5.0$ . The pink color represents the initial conditions for the oscillatory state and light blue for the homogeneous steady state (b) at the death region  $\epsilon_h = 5.6$ . The four distinct colors represent the four choices of fixed points for the system at a steady state. Here  $N = 100$ ,  $\omega = 1$ .  $i = 1, 2, \dots, N$ .

region. We further explore the impact of the parameter  $\omega$  on the dynamics of the *SL* oscillators with 2-simplex interactions. The parameter-space ( $\epsilon_h - \omega$ ) diagram of Fig. 5(a) illustrates that the transition from oscillatory to steady state occurs for  $\omega \leq 1$  via first-order transition. It is important to note that here in HSS, the system may stabilize to any of the four fixed points, as depicted in Fig. 3(b).

#### D. Both pairwise and triadic interactions

We also study a case where *SL* oscillators interact through 1- and 2-simplex interactions. For a weak 1-simplex interaction ( $\epsilon_p \leq 0.8$ ), the system manifests a first-order transition from the oscillatory to the steady state with an increase in  $\epsilon_h$ . For intermittent values,  $1 < \epsilon_p < 0.8$ , a region of bistability or hysteresis is observed regardless of  $\epsilon_h$  values. The system

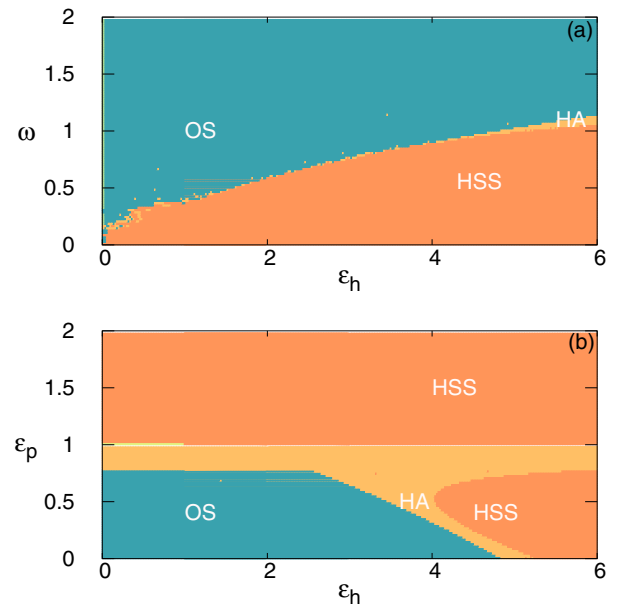


FIG. 5. Different dynamical domains of  $N$  coupled *SL* oscillators are plotted in the parameter plane (a) ( $\epsilon_h - \omega$ ) for  $\epsilon_p = 0$  and (b) ( $\epsilon_h - \epsilon_p$ ) for  $\omega = 1$ . Here OS, HA, and HSS denote oscillatory state, hysteresis area, and homogeneous steady state.

with stronger  $\epsilon_p \geq 1.0$  always attains a steady state and has no additional effect of 2-simplex interaction. Hence, we can conclude that the triadic conjugate interactions lead to more complex dynamics with the first-order transition from oscillatory to steady state in the globally coupled Stuart-Landau oscillators as compared to the second-order transition in the presence of 1-simplex conjugate interaction.

**E. Analytical calculations**

By analyzing Eq. (2) and putting  $\epsilon_h = 0$  along with  $\epsilon_p = \epsilon$  we derive the following stable fixed point:

$$x^* = \sqrt{\frac{1 - \epsilon + \omega - \frac{\omega}{\epsilon} + \eta}{2}}$$

$$y^* = \frac{\epsilon(\epsilon - \omega)(\epsilon + \omega)\sqrt{1 + \omega + \frac{\epsilon^2\eta - \epsilon(\epsilon^2 + \omega)}{\epsilon^2}}}{\sqrt{2}\eta\epsilon^2}, \quad (3)$$

where  $\eta = \frac{\sqrt{\epsilon^2(\epsilon - \omega)^3(\epsilon + \omega)}}{\epsilon^2}$ . To find the condition of the transition from oscillatory to death state, the Jacobian  $\mathcal{W}$  is written in the form of block circulant matrices [57], i.e.,  $\mathcal{J} = \text{circ}(\zeta_1, \zeta_2, \dots, \zeta_2)$ :

$$\zeta_1 = \begin{bmatrix} 1 - \epsilon - 3x^2 - y^2 & \frac{\epsilon}{2} - \omega - 2xy \\ \frac{\epsilon}{2} + \omega - 2xy & 1 - \epsilon - x^2 - 3y^2 \end{bmatrix}$$

and  $\zeta_2 = \begin{bmatrix} 0 & \frac{\epsilon}{2} \\ \frac{\epsilon}{2} & 0 \end{bmatrix}$ .

A  $2(N - 1)$  degeneracy exists for  $2(N - 1)$  eigenvalues of  $\mathcal{W}$ . These eigenvalues are equal to the eigenvalues of the matrix  $(\zeta_1 - \zeta_2)$ . The other eigenvalues of  $\mathcal{W}$  will equal to those of the matrix  $\zeta_1 + (N - 1)\zeta_2$ . The characteristic equation corresponding to the matrix  $\zeta_1 + (N - 1)\zeta_2$  is given by

$$\lambda^2 + d_1\lambda + d_0 = 0, \quad (4)$$

where  $d_1 = -2 + 2\epsilon + 4x^{*2} + 4y^{*2}$  and  $d_0 = 1 - 2\epsilon + \omega^2 - 4x^{*2} + 4\epsilon x^{*2} + 3x^{*4} + 4\epsilon x^*y^* - 4y^{*2} + 6x^{*2}y^{*2} + 3y^{*4}$ . The condition for the Hopf bifurcation point is derived according to the Routh-Hurwitz criterion [58] by putting  $d_1 = 0$ . Hence, the critical value of  $\epsilon$  for the transition of the system from the oscillatory to OD state through Hopf bifurcation is given by

$$\epsilon_{HB} = \frac{1}{3}(-1 + 2\sqrt{1 + 3\omega^2}). \quad (5)$$

The condition for pitchfork bifurcation may also be derived by putting  $d_0 = 0$ :

$$\epsilon_{PB} = \frac{1}{2}(1 + \omega^2). \quad (6)$$

Putting  $\omega = 1$  in Eqs. (5) and (6),  $\epsilon_{HB}$  and  $\epsilon_{PB}$  are both found to be 1, which is in exact agreement with our numerical results.

We analyze Eq. (2) again, and this time by considering only the triadic interactions, i.e.,  $\epsilon_p = 0$  and  $\epsilon_h$  is generalized to  $\epsilon$ . Numerical simulations reflect that the coupled system stabilizes at the HSS. Hence, the backward transition point for the explosive transition can be computed by the stability analysis of HSS. The stable fixed points for this system are,

$x_i^* = x^*, y_i^* = y^*, \forall i = 1, \dots, N$ , where,

$$x^* = \pm \frac{1}{2} \sqrt{\frac{2 + \epsilon + \alpha \pm \sqrt{2}(1 + \epsilon)\beta}}{1 + \epsilon}},$$

$$y^* = \pm \frac{1}{4(1 + \epsilon)\omega} (\pm\epsilon \pm \alpha + \sqrt{2}\epsilon\beta + \sqrt{2}\epsilon^2\beta)x^*, \quad (7)$$

where  $\alpha = \sqrt{\epsilon^2 - 4(1 + \epsilon)\omega^2}$  and  $\beta = \sqrt{\frac{\epsilon + 2\omega^2 + 2\epsilon\omega^2 - \alpha}{\epsilon(1 + \epsilon)^2}}$ .  $2N \times 2N$  Jacobian matrices can be written in the form of block circulant matrices  $\mathcal{J} = \text{circ}(\mathcal{M}_1, \mathcal{M}_2, \dots, \mathcal{M}_2)$ .

$$\mathcal{M}_1 = \begin{bmatrix} 1 - \Omega x^2 + \frac{y^2}{3}\kappa & -\omega + \frac{2}{3}\kappa xy \\ \omega + \frac{2}{3}\kappa xy & 1 - \Omega y^2 + \frac{x^2}{3}\kappa \end{bmatrix} \text{ and } \mathcal{M}_2 = \begin{bmatrix} \frac{\epsilon y^2}{3} & \frac{2\epsilon xy}{3} \\ \frac{2\epsilon xy}{3} & \frac{\epsilon x^2}{3} \end{bmatrix} \text{ with } \Omega = 3(1 + \epsilon) \text{ and } \kappa = (-3 + \epsilon).$$

As explained earlier, there will be  $2(N - 1)$  eigenvalues of  $\mathcal{J}$  with  $2(N - 1)$  degeneracy. These eigenvalues are equal to the eigenvalues of the matrix  $(\mathcal{M}_1 - \mathcal{M}_2)$ . The rest of the eigenvalues will be equal to the eigenvalues of the matrix  $\mathcal{M}_1 + (N - 1)\mathcal{M}_2$  and can be analyzed to know the stability of the HSS state. The characteristic equation corresponding to this matrix is given by

$$\lambda^2 + c_1\lambda + c_0 = 0, \quad (8)$$

where  $c_1 = -2 + 4x^{*2} + 2\epsilon x^{*2} + 4y^{*2} + 2\epsilon y^{*2}$  and  $c_0 = 1 + \omega^2 - 4x^{*2} - 2\epsilon x^{*2} + 3x^{*4} - 3\epsilon^2 x^{*4} - 4y^{*2} - 2\epsilon y^{*2} + 6x^{*2}y^{*2} + 24\epsilon x^{*2}y^{*2} + 6\epsilon^2 x^{*2}y^{*2} + 3y^{*4} - 3\epsilon^2 y^{*4}$ . Solving Eq. (8), we have two eigenvalues:

$$\lambda_{1,2} = \frac{1}{2(1 + \epsilon)}(-2 - 2\epsilon - \epsilon^2 - 2\alpha - \epsilon\alpha \pm \gamma), \quad (9)$$

where  $\gamma = \sqrt{2[2 - 4\alpha + 8\omega^2 + \epsilon(4 + 16\omega^2 - 6\alpha) + \epsilon^2\xi]}$ , where  $\xi = 2 + 6\omega^2 + \epsilon(\alpha + \epsilon - 2\omega^2)$  and  $\alpha = \sqrt{\epsilon^2 - 4(1 + \epsilon)\omega^2}$ . Equating the real parts of the eigenvalues to zero, we obtain the an expression for the backward transition point through saddle-node bifurcation:

$$\epsilon_{SN} = 2(\omega^2 + \sqrt{\omega^2 + \omega^4}). \quad (10)$$

Hence, we confirm that this model system stabilizes to a homogeneous steady state through a saddle-node bifurcation. The calculated backward transition point from Eq. (10) after considering  $\omega = 1$  is found to be 4.82, which agrees with our numerical results.

**F. Effect of noise on model**

We have also checked the robustness of our results in the presence of Gaussian noise. In most real-world systems, stochasticity or noise is omnipresent. To make our model more realistic, we introduce additive noise into the system. Hence, our model equation is modified as follows:

$$\dot{x}_i = (1 - x_i^2 - y_i^2)x_i - \omega y_i + \frac{\epsilon_p}{N} \sum_{j=1}^N (y_j - x_i) + \frac{\epsilon_h}{N^2} \sum_{j=1}^N \sum_{k=1}^N (x_j y_k^2 - x_i^3) + D\xi(t),$$

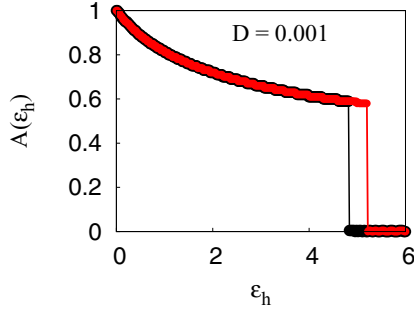


FIG. 6. Order parameter  $A(\epsilon_h)$  computed for 2-simplex with fixed noise strength  $D = 0.001$ . The red curve corresponds to the forward computation, and the black one corresponds to the backward continuation of coupling strength  $\epsilon_h$ . Here,  $\omega = 1$  and  $N = 100$ ,  $\epsilon_p = 0$ .

$$\begin{aligned} \dot{y}_i = & (1 - x_i^2 - y_i^2)y_i + wx_i + \frac{\epsilon_p}{N} \sum_{j=1}^N (x_j - y_i) \\ & + \frac{\epsilon_h}{N^2} \sum_{j=1}^N \sum_{k=1}^N (y_j x_k^2 - y_i^3) + D\xi(t), \end{aligned} \quad (11)$$

where  $\xi(t)$  denotes the Gaussian white noise with zero mean and unit variance with the intensity of the noise signal represented by  $D$ .  $\xi(t) \in \mathbb{R}$  is the additive noise with  $\langle \xi(t) \rangle = 0$  and  $\langle \xi_i(t)\xi_j(t') \rangle = \delta_{ij}\delta(t-t')\forall i, j$ . Equation (11) is integrated using the stochastic Euler-Maruyama scheme with an integration step size of 0.001. The noise is added to the system at each value of  $\epsilon_h$ , as we sweep it in forward and backward continuation. We apply a noise signal of intensity  $D = 0.001$  and observe that the first-order nature of the transition from oscillation to steady state persists. In Fig. 6 the backward and forward continuation diagrams have been denoted by the black and red curves, respectively. The pairwise coupling strength  $\epsilon_p$  has been considered to be 0, while only the 2-simplex coupling strength  $\epsilon_h$  has been varied in the adiabatic way. The backward transition point is noted to be at  $\epsilon_h \approx 4.83$  and the forward transition point is at  $\epsilon_h \approx 5.19$ . Hence we conclude that in the presence of stochastic fluctuations, our model system is robust and the nature of the transition, along with the phenomenon of an abrupt transition to death state remains intact.

## II. CONCLUSION

Here we have investigated the  $SL$  oscillators coupled through conjugate variables and having higher-order interactions. We report the first-order transition, an irreversible

transition from oscillation to steady state, by considering triadic conjugate-coupled interactions instead of the reversible and continuous transition for pairwise conjugate interactions. As expected, triadic connections yield more complex dynamics with the coexistence of oscillatory and steady states in the transition region. We have observed a thin hysteresis region in the parameter space. This region contains two stable states; oscillatory and steady state. This bi-stability in the hysteresis region has important applications in the natural systems where oscillatory and steady states have been found to coexist, such as fruit flies in eclosion rhythm [59] and injection of stimulus pulse to restart the activity in the sino-arterial node [60] among others. After the transition to the steady state, the system stabilizes at four different fixed points, depending on the choice of the initial conditions. We analyzed the basins of attraction in the hysteresis and steady-state regions and confirmed our numerical results analytically by performing linear stability analysis. The analytical calculations have further allowed us to derive the backward transition point that matches the numerical results. We have reported the occurrence of consecutive saddle-node bifurcations at the transition region, leading the system to settle down to HSS. Numerical simulations here have been performed for  $N = 100$ , which match fairly well with the analytical results which are independent of  $N$ . Hence, it is safe to conclude that the results presented here are valid for large-size networks as well. Also, we have demonstrated that the nature of the transition from oscillatory to death state is robust against the addition of finite noise level. The present study can be extended for network topologies such as Erdős-Rényi random networks and small-world networks, etc. Further, this study is restricted to only dyadic and triadic interactions. Including higher-order simplicial structures is a straightforward extension of the present work. A network of heterogeneous oscillators with distributions of intrinsic frequencies  $\omega$  might garner further interesting emerging dynamics in conjugate higher-order coupling. To conclude, the study may be used to understand the origin of hysteresis and oscillation suppression phenomena in biological, ecological, and chemical systems, which have multiple agents interacting and need to be mapped with higher-order interactions.

## ACKNOWLEDGMENTS

R.G. acknowledges financial support from University Grants Commission New Delhi for the SJSGC fellowship. S.J. gratefully acknowledges SERB Power Grant No. SPF/2021/000136 and VAJRA Project No. VJR/2019/000034. M.D.S. acknowledges financial support from SERB, Department of Science and Technology (DST), India (Grant No. CRG/2021/003301).

- [1] R. Pastor-Satorras, C. Castellano, P. Van Mieghem, and A. Vespignani, Epidemic processes in complex networks, *Rev. Mod. Phys.* **87**, 925 (2015).  
 [2] A. R. Benson, D. F. Gleich, and J. Leskovec, Higher-order organization of complex networks, *Science* **353**, 163 (2016).

- [3] D. Centola, J. Becker, D. Brackbill, and A. Baronchelli, Experimental evidence for tipping points in social convention, *Science* **360**, 1116 (2018).  
 [4] A. Sanchez-Gorostiaga, D. Bajić, M. L. Osborne, J. F. Poyatos, and A. Sanchez, High-order interactions distort the functional

- landscape of microbial consortia, *PLoS Biol.* **17**, e3000550 (2019).
- [5] A. Ritz, A. N. Tegge, H. Kim, C. L. Poirel, and T. Murali, Signaling hypergraphs, *Trends Biotechnol.* **32**, 356 (2014).
- [6] G. Petri, P. Expert, F. Turkheimer, R. Carhart-Harris, D. Nutt, P. J. Hellyer, and F. Vaccarino, Homological scaffolds of brain functional networks, *J. R. Soc. Interface.* **11**, 20140873 (2014).
- [7] S. Yu, H. Yang, H. Nakahara, G. S. Santos, D. Nikolić, and D. Plenz, Higher-order interactions characterized in cortical activity, *J. Neurosci.* **31**, 17514 (2011).
- [8] J. Grilli, G. Barabás, M. J. Michalska-Smith, and S. Allesina, Higher-order interactions stabilize dynamics in competitive network models, *Nature (London)* **548**, 210 (2017).
- [9] E. Bairey, E. D. Kelsic, and R. Kishony, High-order species interactions shape ecosystem diversity, *Nat. Commun.* **7**, 12285 (2016).
- [10] S. Boccaletti, P. De Lellis, C. del Genio, K. Alfaro-Bittner, R. Criado, S. Jalan, and M. Romance, The structure and dynamics of networks with higher order interactions, *Phys. Rep.* **1018**, 1 (2023).
- [11] L. M. Pecora and T. L. Carroll, Synchronization in Chaotic Systems, *Phys. Rev. Lett.* **64**, 821 (1990).
- [12] J.-M. Lehn, Toward self-organization and complex matter, *Science* **295**, 2400 (2002).
- [13] A. Koseska, E. Volkov, and J. Kurths, Oscillation quenching mechanisms: Amplitude vs. oscillation death, *Phys. Rep.* **531**, 173 (2013).
- [14] D. M. Abrams and S. H. Strogatz, Chimera States for Coupled Oscillators, *Phys. Rev. Lett.* **93**, 174102 (2004).
- [15] U. K. Verma, A. Sharma, N. K. Kamal, and M. D. Shrimali, First order transition to oscillation death through an environment, *Phys. Lett. A* **382**, 2122 (2018).
- [16] R. Karnatak, R. Ramaswamy, and A. Prasad, Synchronization regimes in conjugate coupled chaotic oscillators, *Chaos* **19**, 033143 (2009).
- [17] R. Arumugam, P. S. Dutta, and T. Banerjee, Environmental coupling in ecosystems: From oscillation quenching to rhythmogenesis, *Phys. Rev. E* **94**, 022206 (2016).
- [18] S. Dixit and M. D. Shrimali, Static and dynamic attractive–repulsive interactions in two coupled nonlinear oscillators, *Chaos* **30**, 033114 (2020).
- [19] G. Saxena, A. Prasad, and R. Ramaswamy, Amplitude death: The emergence of stationarity in coupled nonlinear systems, *Phys. Rep.* **521**, 205 (2012).
- [20] A. Koseska, E. Volkov, and J. Kurths, Parameter mismatches and oscillation death in coupled oscillators, *Chaos* **20**, 023132 (2010).
- [21] G. B. Ermentrout, Oscillator death in populations of “all to all” coupled nonlinear oscillators, *Physica D* **41**, 219 (1990).
- [22] M.-D. Wei and J.-C. Lun, Amplitude Death in Coupled Chaotic solid-state lasers with cavity-configuration-dependent instabilities, *Appl. Phys. Lett.* **91**, 061121 (2007).
- [23] B. Gallego and P. Cessi, Decadal variability of two oceans and an atmosphere, *J. Clim.* **14**, 2815 (2001).
- [24] J. Gómez-Gardeñes, S. Gómez, A. Arenas, and Y. Moreno, Explosive synchronization transitions in scale-free networks, *Phys. Rev. Lett.* **106**, 128701 (2011).
- [25] J. Wang, C. Gu, and P. Ji, Frequency-amplitude correlation inducing first-order phase transition in coupled oscillators, *New J. Phys.* **24**, 073038 (2022).
- [26] N. Bastas, P. Giazitzidis, M. Maragakis, and K. Kosmidis, Explosive percolation: Unusual transitions of a simple model, *Physica A* **407**, 54 (2014).
- [27] U. K. Verma, A. Sharma, N. K. Kamal, J. Kurths, and M. D. Shrimali, Explosive death induced by mean–field diffusion in identical oscillators, *Sci. Rep.* **7**, 7936 (2017).
- [28] H. Bi, X. Hu, X. Zhang, Y. Zou, Z. Liu, and S. Guan, Explosive oscillation death in coupled Stuart–Landau oscillators, *Europhys. Lett.* **108**, 50003 (2014).
- [29] N. Zhao, Z. Sun, X. Yang, and W. Xu, Restoration of oscillation from conjugate-coupling–induced amplitude death, *Europhys. Lett.* **118**, 30005 (2017).
- [30] N. Zhao, Z. Sun, X. Yang, and W. Xu, Explosive death of conjugate coupled van der Pol oscillators on networks, *Phys. Rev. E* **97**, 062203 (2018).
- [31] W. Han, H. Cheng, Q. Dai, H. Li, P. Ju, and J. Yang, Amplitude death, oscillation death, wave, and multistability in identical Stuart–Landau oscillators with conjugate coupling, *Commun. Nonlinear Sci. Numer. Simul.* **39**, 73 (2016).
- [32] A. Sharma, Time delay induced partial death patterns with conjugate coupling in relay oscillators, *Phys. Lett. A* **383**, 1865 (2019).
- [33] N. Zhao, Z. Sun, and W. Xu, Enhancing coherence via tuning coupling range in nonlocally coupled Stuart–Landau oscillators, *Sci. Rep.* **8**, 8721 (2018).
- [34] K. Ponrasu, K. Sathiyadevi, V. Chandrasekar, and M. Lakshmanan, Conjugate coupling-induced symmetry breaking and quenched oscillations, *Europhys. Lett.* **124**, 20007 (2018).
- [35] S. Dutta, O. Alamoudi, Y. S. Vakilina, S. Pati, and S. Jalan, Oscillation quenching in stuart-landau oscillators via dissimilar repulsive coupling, *Phys. Rev. Res.* **5**, 013074 (2023).
- [36] Z. Sun, S. Liu, and N. Zhao, Explosive and semi-explosive death in coupled oscillators, *Chaos, Solitons Fractals* **142**, 110514 (2021).
- [37] R. Herrero, M. Figueras, J. Rius, F. Pi, and G. Orriols, Experimental observation of the amplitude death effect in two coupled nonlinear oscillators, *Phys. Rev. Lett.* **84**, 5312 (2000).
- [38] K. Bar-Eli and S. Reuveni, Stable stationary states of coupled chemical oscillators. experimental evidence, *J. Phys. Chem.* **89**, 1329 (1985).
- [39] F. Parastesh, M. Mehrabbeik, K. Rajagopal, S. Jafari, and M. Perc, Synchronization in Hindmarsh–Rose neurons subject to higher-order interactions, *Chaos* **32**, 013125 (2022).
- [40] M. S. Anwar and D. Ghosh, Stability of synchronization in simplicial complexes with multiple interaction layers, *Phys. Rev. E* **106**, 034314 (2022).
- [41] R. Ghorbanchian, J. G. Restrepo, J. J. Torres, and G. Bianconi, Higher-order simplicial synchronization of coupled topological signals, *Commun. Phys.* **4**, 120 (2021).
- [42] M. Lucas, G. Cencetti, and F. Battiston, Multiorder Laplacian for synchronization in higher-order networks, *Phys. Rev. Res.* **2**, 033410 (2020).
- [43] L. Gallo, R. Muolo, L. V. Gambuzza, V. Latora, M. Frasca, and T. Carletti, Synchronization induced by directed higher-order interactions, *Commun. Phys.* **5**, 263 (2022).
- [44] P. Rajwani, A. Suman, and S. Jalan, Tiered synchronization in Kuramoto oscillators with adaptive higher-order interactions, *Chaos* **33** (2023).

- [45] S. Kundu and D. Ghosh, Higher-order interactions promote chimera states, *Phys. Rev. E* **105**, L042202 (2022).
- [46] P. S. Skardal and A. Arenas, Higher order interactions in complex networks of phase oscillators promote abrupt synchronization switching, *Commun. Phys.* **3**, 218 (2020).
- [47] A. P. Millán, J. J. Torres, and G. Bianconi, Explosive Higher-Order Kuramoto Dynamics on Simplicial Complexes, *Phys. Rev. Lett.* **124**, 218301 (2020).
- [48] S. Jalan and A. Suman, Multiple first-order transitions in simplicial complexes on multilayer systems, *Phys. Rev. E* **106**, 044304 (2022).
- [49] A. D. Kachhah and S. Jalan, First-order route to antiphase clustering in adaptive simplicial complexes, *Phys. Rev. E* **105**, L062203 (2022).
- [50] N. Zhao and X. Zhang, Impact of higher-order interactions on amplitude death of coupled oscillators, *Physica A* **622**, 128803 (2023).
- [51] R. Karnatak, R. Ramaswamy, and A. Prasad, Amplitude death in the absence of time delays in identical coupled oscillators, *Phys. Rev. E* **76**, 035201(R) (2007).
- [52] T. Singla, N. Pawar, and P. Parmananda, Exploring the dynamics of conjugate coupled Chua circuits: Simulations and experiments, *Phys. Rev. E* **83**, 026210 (2011).
- [53] R. Karnatak, R. Ramaswamy, and U. Feudel, Conjugate coupling in ecosystems: Cross-predation stabilizes food webs, *Chaos, Solitons Fractals* **68**, 48 (2014).
- [54] M. Dasgupta, M. Rivera, and P. Parmananda, Suppression and generation of rhythms in conjugately coupled nonlinear systems, *Chaos* **20**, 023126 (2010).
- [55] L. V. Gambuzza, F. Di Patti, L. Gallo, S. Lepri, M. Romance, R. Criado, M. Frasca, V. Latora, and S. Boccaletti, Stability of synchronization in simplicial complexes, *Nat. Commun.* **12**, 1255 (2021).
- [56] V. Resmi, G. Ambika, R. E. Amritkar, and G. Rangarajan, Amplitude death in complex networks induced by environment, *Phys. Rev. E* **85**, 046211 (2012).
- [57] P. J. Davis, *Circulant Matrices* (Wiley, New York, 1979), Vol. 120.
- [58] W.-M. Liu, Criterion of Hopf bifurcations without using eigenvalues, *J. Math. Anal. Appl.* **182**, 250 (1994).
- [59] A. Beuter, L. Glass, M. C. Mackey, and M. S. Titcombe, *Nonlinear Dynamics in Physiology and Medicine* (Springer, New York, 2003).
- [60] M. R. Guevara and H. J. Jongsma, Three ways of abolishing automaticity in sinoatrial node: Ionic modeling and nonlinear dynamics, *Am. J. Physiol. Heart Circ. Physiol.* **262**, H1268 (1992).